2008 IEEE/RSJ International Conference on Intelligent Robots and Systems
Acropolis Convention Center
Nice, France, Sept, 22-26, 2008

Motion Control of Omni-Directional Type Cane Robot Based on Human Intention

Jian Huang, *Member, IEEE*, Pei Di, Toshio Fukuda, *Fellow, IEEE* and Takayuki Matsuno

***Abstract*— A three-wheeled omni-directional cane robot is designed for aiding the elderly walking. Possible move modes are analyzed and a corresponding hybrid model is constructed to describe walking behavior. A concept called intentional direction is presented to denote the moving intention of a human. Based on experiments and some assumptions, dynamic model of intentional direction is obtained as well as its online estimation method. A new admittance control scheme is presented based on intentional direction, which provides natural and intuitive human machine interface. Experiment results show the effectiveness of the design.**

I. Introduction

MANY countries have entered the aging society very rapidly. It is significant to design intelligent robots assisting the elders in daily life. Walker-type support systems are important ones among them because the ability of walk is one of the most fundamental functions for humans.

So far, many researchers have developed various intelligent walkers comprising active or passive wheels and supporting frame. Kotani et al. proposed the Hitomi system to help the blind in outdoor environment [1]. Fujie et al. developed a power-assisted walker for physical support during walking [2]. The Care-O-bot and Nursebot are developed as personal service robots for elderly and disables [3, 4]. Yu et al. proposed the Personal Aid for Mobility and Monitoring (PAMM) system to provide mobility assistance and user health status monitoring [5]. Hirata et al proposed a new intelligent walker based on passive robotics to assist the elderly, handicapped people and the blind [6].

Many elders and patients are not so weak that they have to be nursed carefully. Nevertheless, sufficient support, like a cane or stick, is necessary to help them take a walk outside, which enables them to realize high-quality lives or accelerate the rehabilitation. In these cases, an intelligent cane system may be more useful than walkers due to its flexibility and handiness. In [5], a SmartCane system is also proposed, which has relative smaller size and nonholonomic constraint in kinematics. The nonholonomic constraint is useful for moving along a path stably, but reduces the maneuverability of the system. In the living environment including the narrow space, the cane system is expected to be movable in omni-directions. Thus, omni-directional mobile platform is needed in the robot design. This kind of platform has been considered in some applications [7, 8]. Whereas, their designs are special and not commercially available. Particularly, they are proposed for walker systems but not for cane systems, which are much smaller in size. Recently, commercial omni-wheels are applied in the area of walker systems [9].

In this study, an intelligent cane system is designed based on a commercially available three-wheeled omni-directional platform. A hybrid model is presented to formulate human walk behavior. To model the human intention, an important concept called 'intentional direction' (ITD) is proposed as well as its dynamic model during human walking. Some filtering technologies are used to online estimate the ITD, based on which a new force control scheme called 'intention based admittance control (IBAC)' is proposed to provide a natural and intuitive interface for elderly users.

II. Intelligent Cane Robot System

A. Mechanism of Cane Robot

In this section, we introduce a prototype system of omni-directional type cane robot shown in Fig. 1, which is developed to help elderly walking.

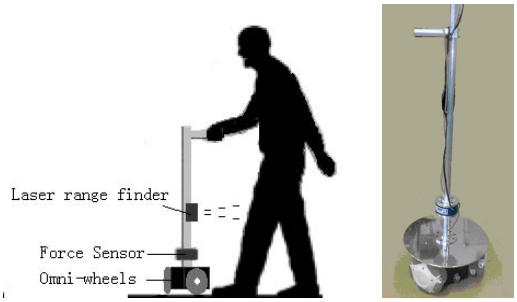

Fig. 1. Prototype of the omni-directional type cane robot

Manuscript received February 23, 2008. This work is a part of the collaboration research work with Shenyang University of Technology (SUT), China. The work of J. Huang was supported by the National Natural Science Foundation of China under Grant 60603006.

J. Huang is with the Department of Micro-Nano Systems Engineering, Nagoya University, Nagoya 464-8603, Japan. He is also with the Department of Control Science and Engineering, Huazhong University of Science and Technology, Hubei 430074, China (e-mail: huang@robo.mein.nagoya-u.ac.jp).

P. Di and T. Fukuda are with the Department of Micro-Nano Systems Engineering, Nagoya University, Nagoya 464-8603, Japan (e-mail: di@robo.mein.nagoya-u.ac.jp, fukuda@mein.nagoya-u.ac.jp).

T. Matsuno is with the Department of Intelligent System Design Engineering, Toyama Prefectural University, Imizu City 939-0398, Japan (e-mail: matsuno@pu-toyama.ac.jp).

The cane robot consists of an omni-directional mobile base, a metal stick and sensor groups including force sensor and laser range finder.

The omni-directional mobile base comprises three commercially available omni-wheels and actuators, which are specially designed for walker systems. Despite the small size, the load capacity of this mobile base is up to 50 kilograms.

The laser range finder measures the distance between the stick and knees of the operator, which plays an important role in the function of fall-prevention [10].

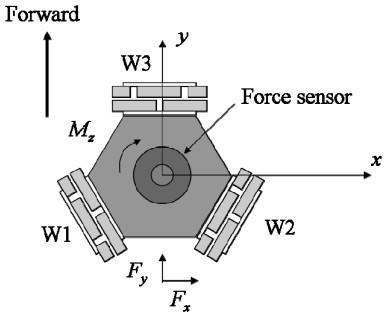

Fig. 2. Arrangement of force sensor and definitions of force signals

A six-axis force/torque sensor attached to the stick is used as the main control input interface. The arrangement and forces definitions are depicted by Fig. 2.

In most of present walker systems, signals from force sensor are interpreted by an admittance controller for motion control. Although the human intention is significant in such applications, conventional admittance control of walker systems does not take it into account explicitly. In this paper, we focus on the motion control problem of the cane robot by explicitly employing online estimated human intention.

B. Control Architecture

There are many possible move modes during the usage of the cane robot. Hirata et al considered three modes including 'normal walking', 'stop' and 'emergency' in their studies [10]. Actually, we can divide these rough modes further. For instance, the mode 'normal walking' consists of 'go straight forward', 'turn left', 'turn right' and so on. Normally, different control scheme is required for different move mode. Considering the high-level *discrete* move modes and low-level motion control scheme based on *continuous* sensor signals, hybrid system theory is selected as the mathematical tool for the modeling and control design. A hierarchical control architecture is also proposed, which is depicted by Fig. 3.

In the high-level supervising module, current move mode is estimated from sensor signals, which is used to choose appropriate filter to infer the human intention. The inferred human intention is taken as the input of the IBAC controller in the low-level motion controller module. All the methods are further illustrated in the following sections.

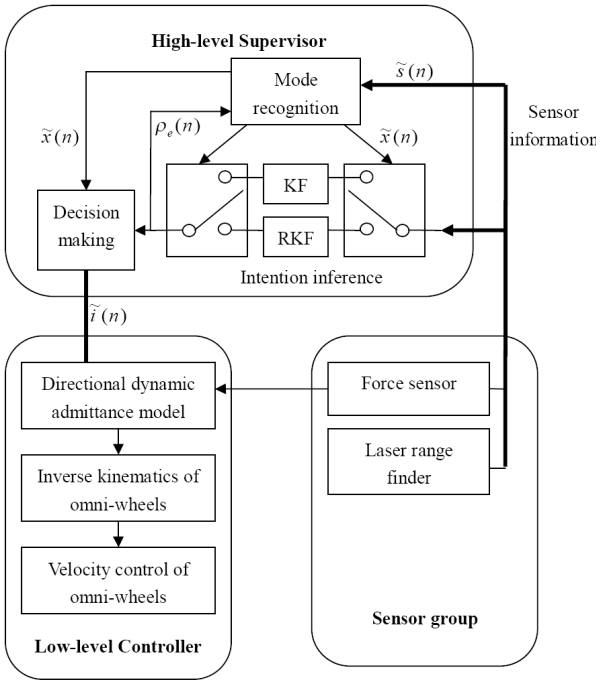

Fig. 3. The hierarchical control structure

III. HIGH-LEVEL SUPERVISOR

A. Modeling for Human Intention

To describe the human intention while using the cane robot, an important concept is defined as follows.

Definition 1. The direction to which a person intends to move is referred to as *intentional direction* (ITD).

As shown by Fig. 4, the ITD can be evaluated by the angle between the forward direction (FW) and the ITD itself. Obviously, the ITD is a time-dependent value and is denoted by $\rho(n)$ in the rest of the paper. Further, the quantity of this intention is characterized by the measured resultant force $F_\rho(n)$ along the ITD. Note that discrete time scale n is assumed for the requirement of filtering technology.

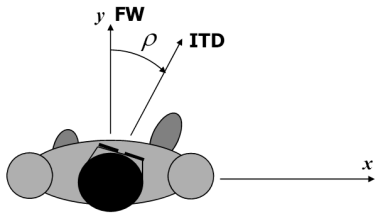

Fig. 4. Top view of a walking person

When the user wants to turn around, it is insufficient to describe human intention only by the ITD. The direction, left or right, to which one wants to turn should be taken into account in this situation. Hence we use a 4-tuple to indicate

the human intention during walking, which is given by

$$\tilde{i}(n) = \left\langle \rho(n), F_\rho(n), T(n), M_T(n) \right\rangle \quad (1)$$

where $T(n) \in \{-1, 0, 1\}$ is used to denote the intended turning direction 'left', 'no turn' and 'right'. $M_T(n)$ is the quantity of the turning intention. In the practice, the absolute value of z-axis moment $|M_z(n)|$ is regarded as the quantity $M_T(n)$.

B. Hybrid System Model of High-level Supervisor

The high-level supervisor monitors the process of walking and online resolve the human intention $\tilde{i}(n)$, which is fed into the low-level IBAC controller.

According to the hybrid system theory, we describe the high-level supervisor by a deterministic finite automaton [11]. This automaton is specified by

$$S = \left(\tilde{S}, \tilde{X}, \tilde{I}, \delta, \phi\right) \quad (2)$$

where $\tilde{S}$ is the set of states, $\tilde{X}$ is the set of move modes, $\tilde{I}$ is the set of resolved human intention, $\delta : \tilde{S} \times \tilde{X} \to \tilde{X}$ is the mode transition function, and $\phi : \tilde{S} \times \tilde{X} \to \tilde{I}$ is the output function.

The state sequence $\{\tilde{s}(n) \mid \tilde{s}(n) \in \tilde{S}\}$ represents the evolution of the continuous sensor signals. At time *t*, the state variable consists of current and previous *m* observations of sensor signals, which is given by

$$\tilde{s}(n) = [F_x(n), F_y(n), M_z(n), F_x(n-1), F_y(n-1), M_z(n-1), \cdots, F_x(n-m), F_y(n-m), M_z(n-m)]^{\mathrm{T}} \quad (3)$$

For simplicity, here we only pay attention to the motion control of normal move modes excluding 'emergency' state. All mode symbols $\tilde{x} \in \tilde{X}$ and the transition diagram are illustrated by Table I and Fig. 5.

The mode transition function δ is realized by rule-based methods. These rules are generated from common-sense experiences. For instance, if previous mode $\tilde{x}(n-1)$ is 'stop' and current forces satisfy

$$F_x(n) \approx 0 \; AND \; F_y(n) > 0 \; AND \; M_z(n) \approx 0,$$

then a transition from 'stop' to 'go straight forward' must have occurred. Due to the length of the paper, we don't list all possible rules here. Fuzzy threshold detection methods are used to check if some rule is satisfied.

C. Inference of Human Intention

The most difficult thing of resolving the human intention $\tilde{i}(n)$ is to estimate the ITD since the turning direction *T*(*n*) can be easily obtained from simple threshold detection of $M_z(n)$. An intuitional method is using the angle between the forward direction and the resultant force of $F_x(n)$ and $F_y(n)$ to represent the ITD. Nevertheless, this method suffers from noisy force signals. Filtering technologies are good choices to obtain accurate enough inference, which necessitates analyzing the dynamics of the ITD.

TABLE I
POSSIBLE WALKING MODES

Mode		Description
I		Stop
II	IIa	Go straight forward
	IIb	Go straight in other directions
III	IIIa	Turn to the right
	IIIb	Turn to the left

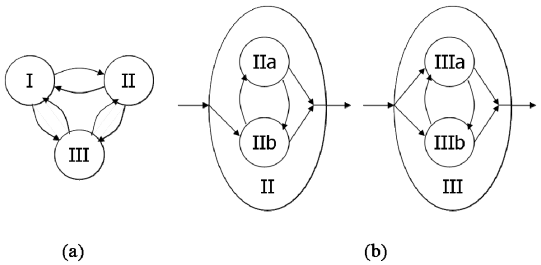

Fig. 5. Transition diagram of possible move modes

In the case of modes 'go straight', including 'go straight forward' and 'go straight in some other direction', we assume the ITD can be characterized by the following discrete linear model:

$$\rho(n+1) = \rho(n) = \rho_0, \quad (4a)$$

$$y(n) = \rho(n) + \omega(n) \quad (4b)$$

where ρ_0 is the initial condition of ITD at the beginning of the current move mode, $y(n)$ is the observation of the ITD which is given by

$$y(n) = \tan^{-1}\left(\frac{F_x(n)}{F_y(n)}\right). \quad (5)$$

$\omega(n)$ is a combination of sensor noises and human gait habit. Everyone has particular gait habit when walking. For example, some people will unintentionally move laterally when they walk straight forward. For simplicity, we assume $\omega(n)$ is a white noise sequence with a direction-dependent covariance $Q(\rho)$ that differs from person to person. For the same person, experiments show that $Q(\rho)$ is almost the same for different directions. This makes it possible to use traditional Kalman filter to estimate the ITD in mode IIa and IIb.

In the case of mode 'turning around', including mode IIIa and IIIb, we assume the ITD is described by

$$\rho(n+1) = a \cdot \rho(n), \quad (6a)$$

$$y(n) = \rho(n) + \omega(n), \quad (6b)$$

where coefficient *a* satisfies $0 < a < 1$, $y(n)$ is the

observation given by (5), $\omega(n)$ is the same as model (4) and it is assumed that the observation noise has the same statistical features for the same person. Model (6) is proposed based on the natural behavior when a person turns around. As shown in Fig. 6, at the beginning of mode IIIa, normally there is a certain target one wants to move, which generates the initial ITD of the mode. During the process of turning around, the value of $\rho(n)$ decreases gradually and finally converges to zero, which causes a transition to mode I or II.

Note that even for the same person, coefficient *a* is uncertain owing to the various locations of target and turning velocities. It is known that traditional Kalman filter will generally not guarantee satisfactory performance when uncertainty exists in the system model. Xie et al proposed a robust Kalman filter which guarantees the filtering error within a certain range [12]. They considered the uncertain dynamic system

$$\begin{aligned} x(n+1) &= [A+\Delta A(n)]x(n)+w(n) \\ y(n) &= [C+\Delta C(n)]x(n)+v(n) \end{aligned} \tag{7}$$

with $x(n)$ denoting the state vector, $y(n)$ the measurement, $w(n)$ the driving disturbance with covariance matrix $W \geq 0$, $v(n)$ the measurement noise with covariance matrix $V \geq 0$ and matrices $\Delta A(n)$ and $\Delta C(n)$ representing the model uncertainty. If the uncertainties satisfy some matching conditions and the system is quadratically stable, then the estimator given by

$$\begin{aligned} \hat{x}(n+1) = A\hat{x}(n) + \left(\overline{A}\overline{Q}\overline{C}^{\mathrm{T}} + M\right)\left(\overline{R} + \overline{C}\overline{Q}\overline{C}^{\mathrm{T}}\right)^{-1} \\ \left(y(n) - \overline{C}\hat{x}(n)\right) \end{aligned} \tag{8}$$

provides a guaranteed steady–state estimation error as given by

$$E\left[\left(x(n)-\hat{x}(n)\right)^{\mathrm{T}}\left(x(n)-\hat{x}(n)\right)\right] \leq \mathrm{trace}(\overline{Q}). \tag{9}$$

The detail of robust Kalman filter can be found in [12] and the estimator (8) can be efficiently solved through LMI toolbox and DARE function in MATLAB.

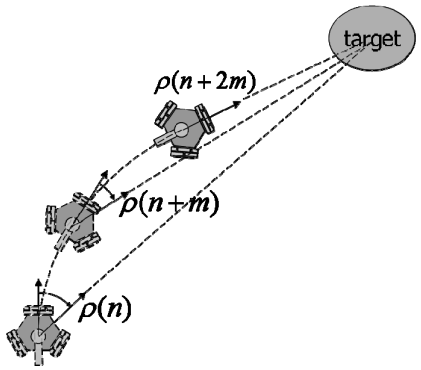

Fig. 6. Typical turning around move mode.

Suppose $a = a_0 + \Delta a(n)$, estimator (8) can then be used to infer the ITD in mode III.

To conclude the above discussion, output function ϕ is implemented by the following algorithm:

Algorithm 1. Intention inference algorithm

Input. $\tilde{s}(n)$, $\tilde{x}(n)$

1. If $\tilde{x}(n-1) = \tilde{x}(n)$ then
2. Switch $\tilde{x}(n)$
3. case I: Let $\tilde{i}(n) = \langle 0,0,0,0 \rangle$
4. case II:
5. Use Kalman filter to infer $\rho(n)$
6. If $\tilde{x}(n) = \mathrm{IIa}$ then let $\rho(n) = 0$
7. Let $\tilde{i}(n) = \langle \rho(n), F_\rho(n), 0, 0 \rangle$
8. case III:
9. Use robust Kalman filter (8) to infer $\rho(n)$
10. Use threshold detection to infer $T(n)$
11. Let $\tilde{i}(n) = \langle \rho(n), F_\rho(n), T(n), |M_z(n)| \rangle$
12. Else
13. Let $\rho(n) = y(n)$, $\tilde{i}(n) = \tilde{i}(n-1)$
14. EndIf

Output: $\tilde{i}(n)$

IV. Low-level motion controller

The low-level motion controller uses a kind of admittance control scheme based on the inferred human intention, which is called intention based admittance control (IBAC) scheme. The conventional admittance control uses an admittance model emulates a dynamic system and gives the user a "feeling" as if he is interacting with the system specified by the model. This model is defined as a transfer function with the user's forces and toques, *F*(*s*), as the input and the reference velocity of cane robot, *V*(*s*), as the output. It is expressed as:

$$G(s) = \frac{V(s)}{F(s)} = \frac{1}{Ms + B} \tag{10}$$

where *M* and *B* are the mass and damping parameters respectively.

A. Intention Based Admittance Control

During walking, people feel comfortable if the cane is easily maneuvered in the ITD and hardly maneuvered in the direction perpendicular to the ITD. To meet the requirement, we propose the IBAC scheme in which two admittance models are used. One model is defined for the motion along the ITD, which has selected mass and damping parameters from the acceptable area presented in [5]. The other model is defined for the motion perpendicular to the ITD, which has much bigger mass and damping parameters. The general

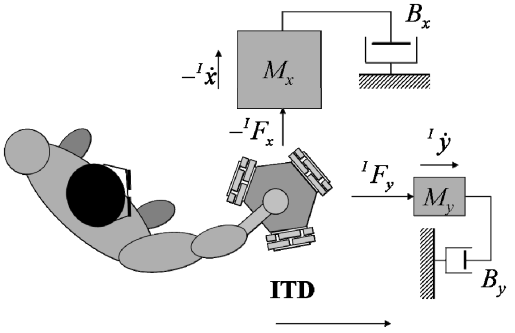

Fig. 7. The principle of IBAC scheme.

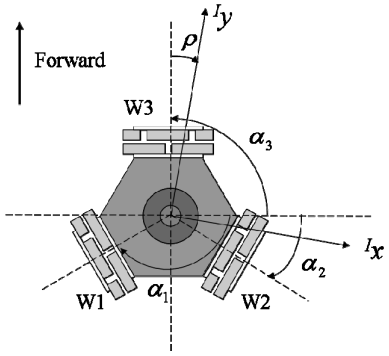

Fig. 8. Coordinate frame {*I*} based on the ITD.

idea is shown by Fig. 7. The final three DOF mass-damping model for our cane robot is defined as:

$$\begin{bmatrix} M_x & 0 & 0 \\ 0 & M_y & 0 \\ 0 & 0 & J_z \end{bmatrix} \begin{bmatrix} {}^I\ddot{x} \\ {}^I\ddot{y} \\ \ddot{\rho} \end{bmatrix} + \begin{bmatrix} B_x & 0 & 0 \\ 0 & B_y & 0 \\ 0 & 0 & B_z \end{bmatrix} \begin{bmatrix} {}^I\dot{x} \\ {}^I\dot{y} \\ \dot{\rho} \end{bmatrix} = \begin{bmatrix} {}^IF_x & {}^IF_y & M_z \end{bmatrix}^{\mathrm{T}} \quad (11)$$

where $M_x >> M_y, J_z$ and $B_x >> B_y, B_z$. The superscript *I* means the variables are defined in the coordinate frame {*I*} based on the current intention, which is depicted in Fig. 8.

B. Kinematics of Three-wheeled Omni-directional Platform

The kinematics of a robot using orthogonal universal wheels separated by 120º have been described previously [13].

Introducing $\xi = \begin{bmatrix} {}^Ix & {}^Iy & \rho \end{bmatrix}^{\mathrm{T}}$ and $\varphi = \begin{bmatrix} \phi_1 & \phi_2 & \phi_3 \end{bmatrix}^{\mathrm{T}}$ to denote the posture in coordinate {*I*} and the angles of three wheels, the kinematics of our omni-directional platform can be described by

$$\dot{\varphi} = \mathbf{R}(\rho) \cdot \dot{\xi} \quad (12)$$

where the rotation matrix **R** satisfies

$$\mathbf{R}(\rho) = \frac{1}{R} \cdot \begin{bmatrix} \sin(\rho - \alpha_1) & -\cos(\rho - \alpha_1) & L \\ \sin(\rho - \alpha_2) & -\cos(\rho - \alpha_2) & L \\ \sin(\rho - \alpha_3) & -\cos(\rho - \alpha_3) & L \end{bmatrix}. \quad (13)$$

As shown in Fig. 8, *R* is the radius of each wheel and *L* is the effective distance between the center of force sensor and the rim of a wheel.

V. Experiments

In this section, we experimented with the cane robot to illustrate the effectiveness of the proposed methods. First, the covariance of the observation noise $\omega(n)$ was investigated. Then the validity of human intention inference algorithm is verified by experiments of three series of move modes.

A. Investigating Covariance of Observation Noise

Two university students utilize the cane robot realizing mode II and III in these experiments. They are requested to intentionally maneuver the robot moving straight along five fixed directions, which is shown by Fig. 9. The results of evaluated covariance $Q(\rho)$ are also depicted in Fig. 9. It is found that values of $Q(\rho)$ are almost the same in different directions for the same person, as pointed out in subsection C of section III.

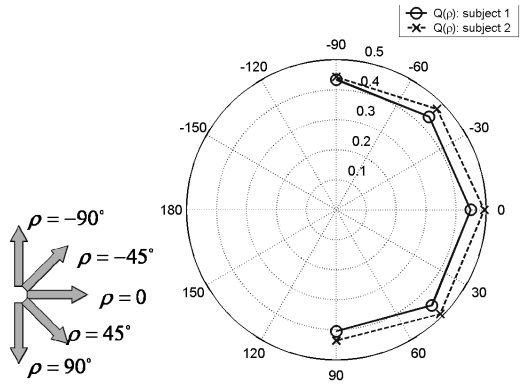

Fig. 9. The covariance of noise when a person moves straight

B. Experiments of Motion Control

In the experiments for illustrating the validity of the hierarchical control architecture, subject A utilized the cane robot to implement two series of move modes.

The inferred ITDs and their observations based on force signals are shown in Fig. 10(a) and Fig. 10(b). Trajectories of estimated mode are also shown in these figures, where we use integers from 1 to 5 to denote the five move modes sequentially. Note that even there are some fault recognitions of mode transition, the performance of rule-based mode transition function δ is sufficiently satisfactory in the practice.

As mentioned above, Kalman filter and robust Kalman filter are used in mode II and III respectively. Coefficient *a*

in model (6) satisfies $a = a_0 + \Delta a(n)$ with $a_0 = 0.93$, $|\Delta a(n)| < 0.3$. Comparing with the observation $y(k)$ from the noisy force signals, the online estimated ITD $\rho_e(k)$ reflects the human intention smoothly and distinctly, which provides explicit guidance to the low-level IBAC controller. In particular, when the subject moves straight forward, which is the move mode in most of the time, the inferred ITD is exactly the forward direction. This reduces meaningless lateral movements of the cane robot to a great extent. Note that the observed ITD $y(k)$ varies severely in the 'stop mode'. This is because in this case the measured x-axial and y-axial forces are nearly zero. The noised force values result in a very uncertain observed ITD in terms of (5).

VI. Conclusion

In this paper, a new omni-directional type cane robot is developed for the elderly. Motion control of this robot is studied based on human intention. Human walking behaviors are modeled by hybrid models and a corresponding hierarchical controller is proposed for the cane robot.

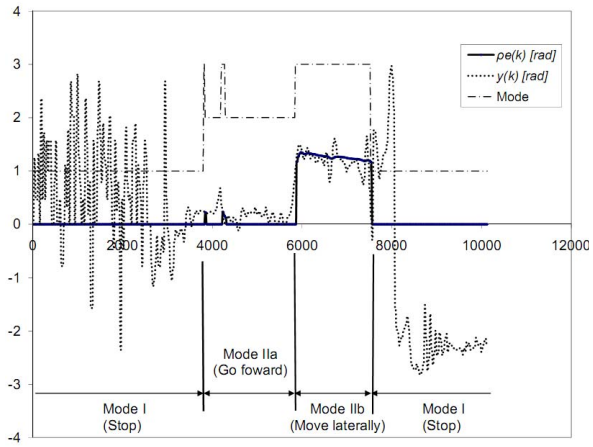

(a) Experiment 1 (I→IIa→IIb→I)

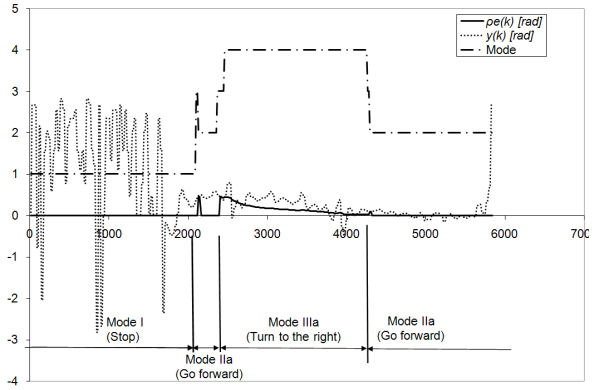

(b) Experiment 2 (I→IIa→IIIa→IIa)

Fig. 10. Observed and inferred ITD vs Time (ms)

The main contribution of this study is to present dynamic models and online inference algorithm for the human intention, which is significant to lead the user walking in a natural and comfortable way. An intention based admittance control (IBAC) scheme is proposed and used to drive the omni-directional mobile base.

Although the cane robot was developed for the elderly, so far experiments were done only for students. An old people may still have physical difficulties of motion even in the ITD. Future work would rely on the adaption of our proposed methods in this serious situation.

References

[1] H. Mori and S. Kotani, "A robotic travel aid for the blind - attention and custom for safe behavior," in International Symposium of Robotics. Research. New York: Springer-Verlag, 1998, pp. 237–245.

[2] M. Fujie, Y. Nemoto, S. Egawa, A. Sakai, S. Hattori, A. Koseki, T. Ishii, "Power assisted walking support and walk rehabilitation", in *Proc. of 1st International Workshop on Humanoid and Human Friendly Robotics*, 1998.

[3] J. Manuel, H. Wandosell, B. Graf, "Non-holonomic navigation system of a walking-aid robot," in *Proc. of IEEE Workshop on Robot and Human Interactive Communication*, 2002, pp. 518-523.

[4] N. Roy, G. Baltus, D. Fox, et al., "Towards personal service robots for the elderly," In *Proc. of the 2000 Workshop on Interactive Robotics and Entertainment (WIRE-2000)*, Pittsburgh.

[5] H. Yu, M. Spenko, S. Dubowsky, "An adaptive shared control system for an intelligent mobility aid for the elderly," *Auton. Robots*, vol.15, no.1, pp.53-66, 2003.

[6] Y. Hirata, A. Hara, and K. Kosuge, "Motion control of passive intelligent walker using servo brakes," *IEEE Trans. Robotics*, vol. 23, no. 5, pp. 981-990, 2007.

[7] H. Yu, S. Dubrowsky, "Omni-directional mobility using active split offset castors," In *Proc. of 2000 ASME IDETC/CIE 26th Biennial Mechanics and Robotics Conference*, Baltimore, Maryland, Sept., 2000. pp. 10-13.

[8] Y. Hirata, T. Baba, K. Kosuge, "Motion control of omni-directional type walking support system "walking helper"," in *Proc. of IEEE Workshop on Robot and Human Interactive Communication*, Nov. 2003, pp. 85-90.

[9] http://www.soai-net.co.jp/service_03.html#omuni

[10] Y. Hirata, A. Muraki and K. Kosuge, "Motion control of intelligent passive-type walker for fall-prevention function based on estimation of user state," in *Proc. of IEEE International Conference on Robotics and Automation*, May, 2006, pp. 3498-3503.

[11] X. D. Koutsoukos, P. J. Antsaklis, J. A. Stiver, et al, "Supervisory control of hybrid systems," *Proceedings of the IEEE*, vol. 88, no. 7, pp. 1026-1049, 2000.

[12] L. Xie, Y. C. Soh, and C. E. de Souza, "Robust Kalman filtering for uncertain discrete-time systems," *IEEE Trans. Automat. Contr.*, vol. 39, no. 6, pp. 1310-1314, 1994.

[13] G. Campion, G. Baskin, and B. D'Andrea-Novel, "Structural properties and classification of kinematic and dynamic models of wheeled mobile robots," *IEEE Trans. Robotics and Automation*, vol. 12, no. 1, pp. 47-62, 1996.